

Mehdi Mazaheri

List of Publications by Year in descending order

Source: <https://exaly.com/author-pdf/1758592/publications.pdf>

Version: 2024-02-01

67
papers

2,742
citations

185998

28
h-index

182168

51
g-index

68
all docs

68
docs citations

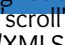
68
times ranked

3162
citing authors

| # | ARTICLE | IF | CITATIONS |
|----|--|-----|-----------|
| 1 | Densification and grain growth of nanocrystalline 3Y-TZP during two-step sintering. <i>Journal of the European Ceramic Society</i> , 2008, 28, 2933-2939. | 2.8 | 152 |
| 2 | Preparation of ZnO nanoparticles from [bis(acetylacetonato)zinc(II)]â€œoleylamine complex by thermal decomposition. <i>Materials Letters</i> , 2008, 62, 1890-1892. | 1.3 | 134 |
| 3 | Preparation of cobalt nanoparticles from [bis(salicylidene)cobalt(II)]â€œoleylamine complex by thermal decomposition. <i>Journal of Magnetism and Magnetic Materials</i> , 2008, 320, 575-578. | 1.0 | 133 |
| 4 | Flexible bactericidal graphene oxideâ€œchitosan layers for stem cell proliferation. <i>Applied Surface Science</i> , 2014, 301, 456-462. | 3.1 | 126 |
| 5 | Multi-walled carbon nanotube/nanostructured zirconia composites: Outstanding mechanical properties in a wide range of temperature. <i>Composites Science and Technology</i> , 2011, 71, 939-945. | 3.8 | 121 |
| 6 | Synthesis of Mn ₃ O ₄ nanoparticles by thermal decomposition of a [bis(salicylidiminato)manganese(II)] complex. <i>Polyhedron</i> , 2008, 27, 3467-3471. | 1.0 | 120 |
| 7 | Preparation of NiO nanoparticles from metal-organic frameworks via a solid-state decomposition route. <i>Inorganica Chimica Acta</i> , 2009, 362, 3691-3697. | 1.2 | 120 |
| 8 | Synthesis and characterization of ZnS nanoclusters via hydrothermal processing from [bis(salicylidene)zinc(II)]. <i>Journal of Alloys and Compounds</i> , 2009, 470, 502-506. | 2.8 | 116 |
| 9 | Effect of a novel sintering process on mechanical properties of hydroxyapatite ceramics. <i>Journal of Alloys and Compounds</i> , 2009, 471, 180-184. | 2.8 | 101 |
| 10 | Reverse precipitation synthesis and characterization of CeO ₂ nanopowder. <i>Journal of Alloys and Compounds</i> , 2010, 491, 499-502. | 2.8 | 97 |
| 11 | Suppression of grain growth in sub-micrometer alumina via two-step sintering method. <i>Journal of the European Ceramic Society</i> , 2009, 29, 1371-1377. | 2.8 | 93 |
| 12 | Two-step sintering of nanocrystalline 8Y ₂ O ₃ stabilized ZrO ₂ synthesized by glycine nitrate process. <i>Ceramics International</i> , 2009, 35, 13-20. | 2.3 | 88 |
| 13 | Master sintering curves of a nanoscale 3Y-TZP powder compacts. <i>Ceramics International</i> , 2009, 35, 547-554. | 2.3 | 82 |
| 14 | Processing of yttria stabilized zirconia reinforced with multi-walled carbon nanotubes with attractive mechanical properties. <i>Journal of the European Ceramic Society</i> , 2011, 31, 2691-2698. | 2.8 | 80 |
| 15 | Processing of nanocrystalline 8mol% yttria-stabilized zirconia by conventional, microwave-assisted and two-step sintering. <i>Materials Science & Engineering A: Structural Materials: Properties, Microstructure and Processing</i> , 2008, 492, 261-267. | 2.6 | 79 |
| 16 | Sintering of titania nanoceramic: Densification and grain growth. <i>Ceramics International</i> , 2009, 35, 685-691. | 2.3 | 78 |
| 17 | Electrodeposition of graphite-brass composite coatings and characterization of the tribological properties. <i>Surface and Coatings Technology</i> , 2001, 148, 71-76. | 2.2 | 64 |
| 18 | Synthesis, characterization and magnetic properties of NiS _{1+x} nanocrystals from [bis(salicylidene)nickel(II)] as new precursor. <i>Materials Research Bulletin</i> , 2009, 44, 2246-2251. | 2.7 | 61 |

| # | ARTICLE | IF | CITATIONS |
|----|---|-----|-----------|
| 19 | Stable Plasmonic-Improved dye Sensitized Solar Cells by Silver Nanoparticles Between Titanium Dioxide Layers. <i>Electrochimica Acta</i> , 2015, 152, 101-107. | 2.6 | 55 |
| 20 | Evaluation of management practices on agricultural nonpoint source pollution discharges into the rivers under climate change effects. <i>Science of the Total Environment</i> , 2022, 838, 156643. | 3.9 | 54 |
| 21 | Wear and friction characteristics of electrodeposited graphite-bronze composite coatings. <i>Surface and Coatings Technology</i> , 2005, 190, 32-38. | 2.2 | 49 |
| 22 | Location and release time identification of pollution point source in river networks based on the Backward Probability Method. <i>Journal of Environmental Management</i> , 2016, 180, 164-171. | 3.8 | 47 |
| 23 | Prediction of electrical conductivity of polymer-graphene nanocomposites by developing an analytical model considering interphase, tunneling and geometry effects. <i>Composites Communications</i> , 2020, 21, 100364. | 3.3 | 45 |
| 24 | Electrodeposition of graphite-bronze composite coatings and study of electroplating characteristics. <i>Surface and Coatings Technology</i> , 2004, 187, 293-299. | 2.2 | 43 |
| 25 | Hot pressing of nanocrystalline zinc oxide compacts: Densification and grain growth during sintering. <i>Ceramics International</i> , 2009, 35, 991-995. | 2.3 | 34 |
| 26 | A developed theoretical model for effective electrical conductivity and percolation behavior of polymer-graphene nanocomposites with various exfoliated filleted nanoplatelets. <i>Carbon</i> , 2020, 169, 264-275. | 5.4 | 32 |
| 27 | Enhanced electrical conductivity of ultrafine-grained 8Y2O3 stabilized ZrO2 produced by two-step sintering technique. <i>Journal of Alloys and Compounds</i> , 2010, 494, 362-365. | 2.8 | 31 |
| 28 | Mathematical Model for Pollution Source Identification in Rivers. <i>Environmental Forensics</i> , 2015, 16, 310-321. | 1.3 | 31 |
| 29 | Microstructural evolution of a commercial ultrafine alumina powder densified by different methods. <i>Journal of the European Ceramic Society</i> , 2011, 31, 2593-2599. | 2.8 | 30 |
| 30 | The Effect of Conformation Method and Sintering Technique on the Densification and Grain Growth of Nanocrystalline 8 mol% Ytria-stabilized Zirconia. <i>Journal of the American Ceramic Society</i> , 2009, 92, 990-995. | 1.9 | 26 |
| 31 | High/room temperature mechanical properties of 3Y-TZP/CNTs composites. <i>Ceramics International</i> , 2014, 40, 3347-3352. | 2.3 | 25 |
| 32 | Electrical behavior of nano-polycrystalline (La _{1-x} Y _x) _{0.7} Ba _{0.3} MnO ₃ manganites. <i>Journal of Magnetism and Magnetic Materials</i> , 2010, 322, 3255-3261. | 1.0 | 23 |
| 33 | Introducing a general framework for pollution source identification in surface water resources (theory and application). <i>Journal of Environmental Management</i> , 2019, 248, 109281. | 3.8 | 21 |
| 34 | Inverse modeling of contaminant transport for pollution source identification in surface and groundwaters: a review. <i>Groundwater for Sustainable Development</i> , 2021, 15, 100651. | 2.3 | 21 |
| 35 | Sintering behavior of nano alumina powder shaped by pressure filtration. <i>Ceramics International</i> , 2011, 37, 9-14. | 2.3 | 20 |
| 36 | Processing, phase evaluation and mechanical properties of MoSi ₂ doped 4Ta-HfC based UHTCs consolidated by spark plasma sintering. <i>International Journal of Refractory Metals and Hard Materials</i> , 2016, 56, 1-7. | 1.7 | 20 |

| # | ARTICLE | IF | CITATIONS |
|----|---|-----|-----------|
| 37 | Preparation and characterization of nano-polycrystalline lanthanum-based manganite. <i>Physica B: Condensed Matter</i> , 2010, 405, 72-76. | 1.3 | 19 |
| 38 | Investigating the restoration of Lake Urmia using a numerical modelling approach. <i>Journal of Great Lakes Research</i> , 2019, 45, 87-97. | 0.8 | 19 |
| 39 | Tunable optical response and fast (slow) light in optomechanical system with phonon pump. <i>Physics Letters, Section A: General, Atomic and Solid State Physics</i> , 2022, 442, 128181. | 0.9 | 19 |
| 40 | Sintering behavior of an ultrafine alumina powder shaped by pressure filtration and dry pressing. <i>Materials Science & Engineering A: Structural Materials: Properties, Microstructure and Processing</i> , 2010, 527, 3807-3812. | 2.6 | 18 |
| 41 | Finite elements based approaches for the modelling of radial crack formation upon Vickers indentation in silicon nitride ceramics. <i>Journal of the European Ceramic Society</i> , 2019, 39, 4011-4022. | 2.8 | 18 |
| 42 | The effect of processing conditions on the microstructure and impact behavior of melt infiltrated Al/SiCp composites. <i>Ceramics International</i> , 2011, 37, 3335-3341. | 2.3 | 17 |
| 43 | In vitro biocompatibility and ageing of 3Y-TZP/CNTs composites. <i>Ceramics International</i> , 2015, 41, 12773-12781. | 2.3 | 16 |
| 44 | A comprehensive one-dimensional numerical model for solute transport in rivers. <i>Hydrology and Earth System Sciences</i> , 2017, 21, 99-116. | 1.9 | 16 |
| 45 | Controllable Synthesis of Covellite Nanoparticles via Thermal Decomposition Method. <i>Journal of Cluster Science</i> , 2016, 27, 593-602. | 1.7 | 15 |
| 46 | Solving Inverse Problems of Unknown Contaminant Source in Groundwater-River Integrated Systems Using a Surrogate Transport Model Based Optimization. <i>Water (Switzerland)</i> , 2020, 12, 2415. | 1.2 | 15 |
| 47 | Processing and impact behavior of Al/SiCp composites fabricated by the pressureless melt infiltration method. <i>Ceramics International</i> , 2009, 35, 1919-1926. | 2.3 | 14 |
| 48 | Field-assisted/spark plasma sintering behavior of CNT-reinforced zirconia composites: A comparative study between model and experiments. <i>Journal of the European Ceramic Society</i> , 2015, 35, 4241-4249. | 2.8 | 12 |
| 49 | Thermal decomposition of [bis(salicylaldehydato)cadmium(II)] to CdS nanocrystals. <i>Polyhedron</i> , 2009, 28, 3975-3978. | 1.0 | 11 |
| 50 | Management scenarios methodology for salinity control in rivers (case study: Karoon River, Iran). <i>Journal of Water Supply: Research and Technology - AQUA</i> , 2019, 68, 74-86. | 0.6 | 11 |
| 51 | Simultaneous synthesis and single-step sintering of lead magnesium niobate ceramic using mixed nanopowders. <i>Ceramics International</i> , 2009, 35, 1139-1144. | 2.3 | 10 |
| 52 | Analytical study on the incorporation of zirconia-based ceramics with carbon nanotubes: Dispersion methods and mechanical properties. <i>Ceramics International</i> , 2016, 42, 1653-1659. | 2.3 | 8 |
| 53 | 3D characterisation of indentation induced sub-surface cracking in silicon nitride using FIB tomography. <i>Journal of the European Ceramic Society</i> , 2019, 39, 3620-3626. | 2.8 | 8 |
| 54 | Mapping QTL for Fusarium head blight resistance in a tunisian-derived durum wheat population. <i>Cereal Research Communications</i> , 2019, 47, 78-87. | 0.8 | 7 |

| # | ARTICLE | IF | CITATIONS |
|----|---|-----|-----------|
| 55 | Introducing a new method for calculating the spatial and temporal distribution of pollutants in rivers. <i>International Journal of Environmental Science and Technology</i> , 2021, 18, 3777-3794. | 1.8 | 7 |
| 56 | A comparison of He and Ne FIB imaging of cracks in microindented silicon nitride. <i>Materials Characterization</i> , 2018, 141, 362-369. | 1.9 | 6 |
| 57 | High Temperature Mechanical Spectroscopy Study of 3 mol% Yttria Stabilized Tetragonal Zirconia Reinforced with Carbon Nanotubes. <i>Solid State Phenomena</i> , 0, 184, 265-270. | 0.3 | 5 |
| 58 | Epidermal growth factor receptor gene expression evaluation in colorectal cancer patients. <i>Indian Journal of Cancer</i> , 2014, 51, 358. | 0.2 | 4 |
| 59 | High-Temperature Mechanical Spectroscopy of Nitrogen-Rich Ca- \pm -SiAlON Ceramics. <i>Journal of the American Ceramic Society</i> , 2011, 94, 1536-1545. | 1.9 | 3 |
| 60 | The effect of neglecting spatial variations of the parameters in pollutant transport modeling in rivers. <i>Environmental Fluid Mechanics</i> , 2021, 21, 587-603. | 0.7 | 3 |
| 61 | Mathematical model of solute transport in rivers with storage zones using nonlinear dispersion flux approach. <i>Hydrological Sciences Journal</i> , 2022, 67, 1656-1668. | 1.2 | 3 |
| 62 | Two-dimensional mechanism of electrical conductivity in Gd $1\hat{a}$ \sim xCe x Ba 2 Cu 3 O $7\hat{a}$ \sim 1. <i>Journal of Physics Condensed Matter</i> , 2008, 20, 345221. | 0.7 | 2 |
| 63 | An innovative framework for real-time monitoring of pollutant point sources in river networks. <i>Stochastic Environmental Research and Risk Assessment</i> , 2022, 36, 1791-1818. | 1.9 | 2 |
| 64 | Structural and electrical transport properties of hexagonal 4H BaRu $1\hat{a}$ \sim xMnxO 3 perovskite. <i>Physica B: Condensed Matter</i> , 2011, 406, 3363-3366. | 1.3 | 1 |
| 65 | Shoreline spatial and temporal response to natural and human effects in Boujagh National Park, Iran. <i>International Journal of Sediment Research</i> , 2021, 36, 582-592. | 1.8 | 1 |
| 66 | Effect of Ca substitution on crystal structure and superconducting properties of ferromagnetic superconductor RuSr $2\hat{a}$ \sim xCa x Gd 1.4 Ce 0.6 Cu 2 .  \langle mml:math altimg="si0030.gif" overflow="scroll" xmlns:xocs="http://www.elsevier.com/xml/xocs/dtd" xmlns:xs="http://www.w3.org/2001/XMLSchema" xmlns:xsi="http://www.w3.org/2001/XMLSchema-instance" xmlns="http://www.elsevier.com/xml/ja/dtd" xmlns:ja="http://www.elsevier.com/xml/ja/dtd" xmlns:mml="http://www.w3.org/1998/Math/MathML" xmlns:tb="http://www.elsevier.com/xml/common/ta. <i>Journal of Magnetism and Magnetic Materials</i> , 2011, 312, 100-105. | 1.0 | 0 |
| 67 | Level shifting circuit for hybrid superconductor-to-semiconductor interface. <i>Physica C: Superconductivity and Its Applications</i> , 2018, 552, 57-60. | 0.6 | 0 |